https://doi.org/10.1016/j.buildenv.2017.08.010

This is the Pre-Published Version.

Experimental study on dehumidification performance enhancement by TiO_2 superhydrophilic coating for liquid desiccant plate dehumidifiers

Chuanshuai Dong, Lin Lu *, Tao Wen

Department of Building Services Engineering, The Hong Kong Polytechnic University, Kowloon, Hong Kong SAR, China

**Corresponding email: vivien.lu@polyu.edu.hk*

Tel.: +852 3400 3596; fax: +852 2774 6146.

© 2017. This manuscript version is made available under the CC-BY-NC-ND 4.0 license https://creativecommons.org/licenses/by-nc-nd/4.0/

Abstract

Liquid desiccant air dehumidification is a promising dehumidification technology with lower energy consumption, less pollution and more flexible humidity control. However, the incomplete wetting conditions of liquid desiccant deteriorates the dehumidification performance and limits the development. Therefore, how to enhance the surface wettability is critical to improving the dehumidification performance as well as reducing the building energy consumption. In this paper, a novel TiO_2 superhydrophilic coating was applied in a plate dehumidifier to enhance the surface wettability and improve the dehumidification performance. Firstly, the characterization of the coating was conducted. The test results showed the surface wettability was effectively improved with the contact angle dramatically decreasing from 84.6° to 8.8°. Then two single-channel internally-cooled liquid desiccant dehumidifiers were fabricated to investigate the effect of TiO_2 coating on dehumidification performance. The experimental results indicated that the dehumidification performance was significantly enhanced with the mean enhancing ratios of 1.60 and 1.63 for moisture removal rate and dehumidification efficiency, respectively. Besides, the influencing factors on dehumidification performance were analysed comprehensively. Based on the analysis, a new empirical correlation of mass transfer coefficient was developed with contact angles considered to reflect the effect of surface wettability on dehumidification performance. Lastly, the energy consumption of liquid desiccant air-conditioning system with coated dehumidifiers for a commercial building in Hong Kong was simulated and around 80 MW·h of the electricity consumption could be saved. This study is helpful to researchers and engineers who are interested in enhancing the dehumidification performance and reducing the building energy consumption.

Keywords: liquid desiccant air dehumidification; incomplete wetting conditions; superhydrophilic coating; dehumidification performance; energy consumption

Nomenclature

A	Wetting area	m^2	ω	Humidity ratio	g/kg
C_p	Specific heat capacity	$kJ/(kg\cdot K)$	$\Delta\omega$	Humidity difference	g/kg
h	Enthalpy	kJ/kg	***Subscripts***		
h_D	Mass transfer coefficient	$g/(m^2\cdot s)$	a	Air	
H	Height	mm	coated	Coated plate	
L	Length	mm	equ	Equilibrium status	
m	Mass flow rate	kg/s	exp	Experimental	
m_ω	Moisture removal rate	g/s	f	Cooling water	
T	Temperature	℃	in	Inlet	
U	Uncertainty		out	Outlet	
W	Width	mm	pre	Predicted	
α	Contact angle	°, rad	s	Solution	
ε_η	Enhancing ratio of dehumidification efficiency		uncoated	Uncoated plate	
ε_ω	Enhancing ratio of moisture removal rate		ω	Humidity	
η_ω	Dehumidification efficiency				

1. Introduction

The building energy consumption has increased rapidly during the past decades [1]. In developed countries, the global contribution from buildings towards energy consumption, both residential and commercial, had steadily increased reaching figures between 20% and 40% and exceeded the major sectors: industry and transportation [2]. Among the building energy services, the Heating, Ventilation and Air-Conditioning (HVAC) systems are the most energy consuming services, accounting for more than 50% of the total building energy consumption. It was reported that the energy consumed by air-conditioning systems took up 54% and 23% of the total building energy consumption for the typical official and residential buildings, respectively, in hot and humid regions, like Hong Kong [3].

In traditional vapor compressor air-conditioning system, the process air is overcooled below the dew point to remove the extra moisture by condensation and sometimes needs to be reheated again to the required supply temperature, which wastes a lot of energy. In addition, the condensation process also provides breeding conditions for the molds and bacterial, leading to potential health issues. Therefore, new air-conditioning technologies are required. The liquid desiccant air-conditioning (LDAC) system is developed and regarded as a promising alternative for lower energy consumption, less pollution and more flexible humidity control [4, 5]. In LDAC systems, the extra moisture is removed by liquid desiccant absorption and the sensible and latent heat can be handled separately. In addition, the regeneration of the weak desiccant solution can be driven by solar energy or industrial waste heat, which can further reduce the energy consumption of air-conditioning systems [6].

The dehumidifier is one of the core components in LDAC systems. The internally-cooled plate dehumidifier is widely used for lower air pressure loss and less possibility of droplets carryover. In internally-cooled plate dehumidifier, the latent heat released during the absorption process is removed by the cooling unit, which can improve the dehumidification performance and reduce the device volume [7]. The investigation of the internally-cooled liquid desiccant dehumidifier has been carried out by many researchers [8-12]. As the dehumidification performance is critical to LDAC system, many researchers have developed various methods to improve the performance [13-26]. These methods can be mainly divided into the following categories, surface treatment [13-17], addition of surfactant or nano-particles [18-23] and structure modification of dehumidifiers [24-26].

Yang and Chou [13] investigated the heat and mass transfer characteristics of absorption process for the falling film flow inside a porous medium and found that the porous medium could significantly enhance the heat and mass transfer performance. Kim et al. [14] studied the effect of micro-scale surface treatment on absorption performance for a falling film LiBr aqueous solution absorber and indicated that the surface treatment could improve the wettability and therefore increase the heat and mass transfer rates. Yin et al. [15] conducted experimental study on absorption performance in falling film outside the vertical tube for water vapor absorption into LiBr aqueous solution. The experimental results showed that the absorption rate was significantly improved by the enhanced tubes. In addition, Zheng et al. [16] adopted superhydrophilic horizontal tubes to enhance the falling film evaporating rates at low spray density. Dong et al. [17] theoretically found that reducing the contact angles could increase the wetting area of desiccant solution on the working plate and in consequence improve the dehumidification performance.

Hihara and Saito [18] used 2-ethyl-1-hexanol as the additive in LiBr aqueous solution and the experimental results showed that the absorption rate was improved four- to five-fold. Cheng et al. [19] investigated the effect of two surfactants, 2-ethyl-1-hexnaol and 1-octanol, on the heat transfer performance in a falling film absorber. The results indicated that the heat transfer rate could be improved up to 100% with optimum concentration. Kang et al. [20] used triton X 100 surfactant (500 ppm) in water and observed that the wetting area could be improved by 34%. Hoffman et al. [21] adopted 2-ethyl-1-hexanol with 80 ppm in a falling film tower and found that the mass transfer coefficient was improved by 60-140%. In addition, Ma et al. [22] investigated the heat and mass transfer enhancement of the bubble absorption using CNTs-NH_3 binary nano-fluid. Patil et al. [23] developed a falling film tower with polypropylene plate using sodium lauryl sulfate-SLS as surfactant addition and the results showed that the improvement of 50% in wettability was achieved.

Schwarzer et al. [24] adopted a novel design of heat and mass transfer exchanger where the working fluid flowed as a thin film on a spirally wound fin formed on the inner wall of a circular tube. Islam et al. [25] developed a novel film-inverting design concept for falling film absorbers and both surfaces of the falling film was alternatively cooled in a periodic manner. The experimental results indicated that the vapor absorption rate could be improved up to 100%. In addition, Cui et al. [26] also proposed a new film-inverting structure for a plate falling film absorber and developed a mathematical model to predict the absorption rates.

In this study, a novel nanoscale titanium dioxide (TiO_2) superhydrophilic coating was applied on the plate dehumidifier to improve the surface wettability. The characterization of the superhydrophilic coating was conducted firstly. Then, two single-channel internally-cooled plate dehumidifiers were fabricated to investigate the effect of superhydrophilic coating on dehumidification performance. Besides, the influencing factors such as inlet parameters of air, liquid desiccant and cooling water on dehumidification performance were comprehensively analysed in this study. Based on the experimental results, an empirical correlation of mass transfer coefficient was developed using nonlinear regression method. In the new correlation, the contact angle was considered to account for the effect of surface wettability on the dehumidification performance. Lastly, the energy consumption of LDAC system with coated plate dehumidifiers for a typical commercial building in Hong Kong was simulated.

2. Experimental test rig

Two single-channel internally-cooled liquid desiccant dehumidifiers were fabricated in this study, as shown in Fig. 1. The photograph of the experimental setup was provided in Fig. 2. Two stainless steel plates were selected as the substrate plates for good heat conductivity and corrosion resistance. Lithium Chloride (LiCl) aqueous was chosen as the absorption medium in this experiment. In Channel Ⅰ, the substrate plate was just cleaned with ethanol, while in Channel Ⅱ, the substrate plate was firstly cleaned with ethanol and then coated with nanoscale TiO_2 superhydrophilic particles. The size of the plate dehumidifier was $550\times100\times600$ mm $(L\times W\times H)$. As shown in Fig. 1, the red line represents the circulation of the liquid desiccant aqueous solution. The desiccant solution was stored in the solution tank and pumped to the inlet of the plate dehumidifier. A new solution distributor was designed to achieve the even distribution of the desiccant falling film, as shown in Fig. 3. After interacting with the process air, the weak desiccant aqueous solution was collected and returned to the solution tank. The green line represents the flow of the process air. The air, supplied by a fan, was firstly heated and humidified to the test condition, and then interacted with the liquid desiccant falling film. The sampling devices were fixed at both inlet and outlet of the air channel to measure the temperature and humidity of the process air. The blue line stands for the circulation of the cooling water. The cooling water was provided by a chiller and used to remove the latent heat released during the absorption process and therefore prevent the temperature increase of the desiccant solution. In addition, the whole channel was well insulated to prevent the heat exchange between the dehumidifiers and the surroundings. The experiment of these two single-channel plate dehumidifiers were conducted simultaneously to ensure the same experimental conditions.

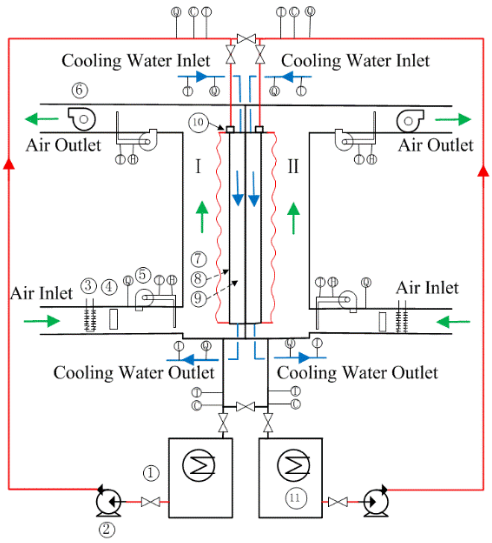

1、Solution tank 2、Solution pump 3、Air heater 4、Humidifier 5、Sampling fan 6、Fan
7、Air channel 8、Working surface 9、Internally cooling unit 10、Solution distributor 11、Heat exchanger
(T) Temperature Sensor (C) Density Sensor (Q) Flowmeter (H) Wet-bulb temperature sensor

Fig. 1. Schematic of the experimental setup

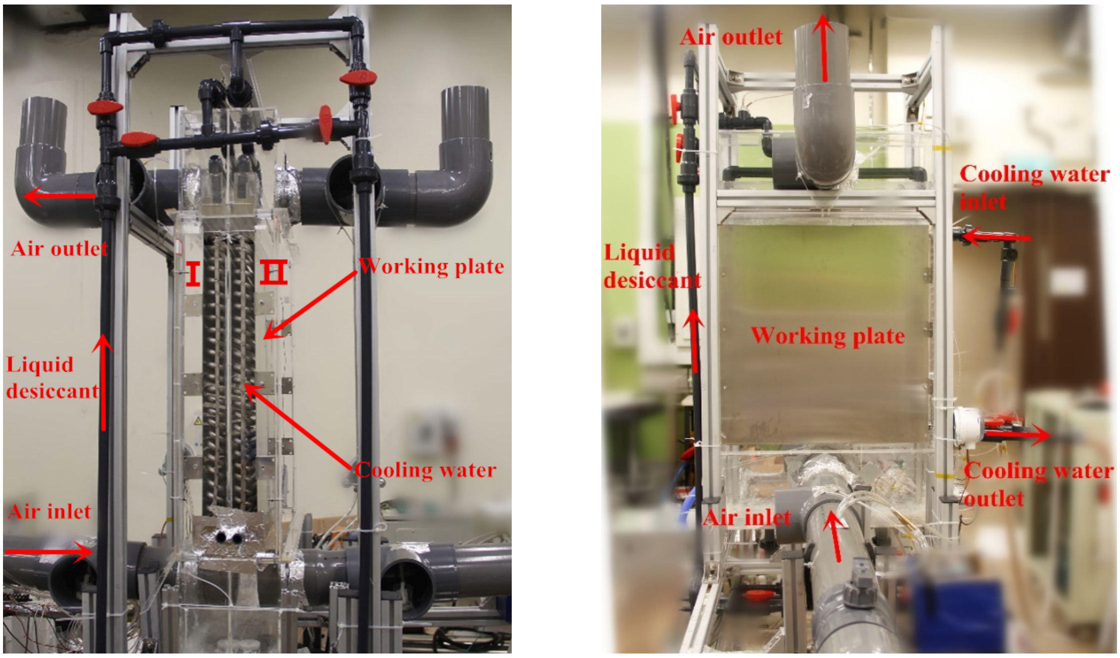

(a) Side view (b) Front view

Fig. 2. Photograph of the experimental setup

Fig. 3 shows the schematic of the newly-designed solution distributor. Three entrance holes were set up at the top of the distributor to ensure the even inlet of the desiccant solution. It was observed that some eddies occurred as the desiccant solution flowed from the inlet pipe to the chamber of the distributor. These eddies could lead to unstable solution levels, which seriously affected the distribution of the desiccant solution. To reduce effect of the solution eddies on the solution distribution, a baffle was installed inside the distributor which separated the chamber into two parts. The desiccant solution firstly flowed into and accumulated in Chamber Ⅰ.When the solution level was above the baffle, the solution began to flow over the baffle smoothly. The effect of the solution eddies was effectively eliminated by the baffle. In addition, an outlet slot was opened in Chamber Ⅱand the even distribution of the falling film could be achieved once the solution level was above the outlet slot.

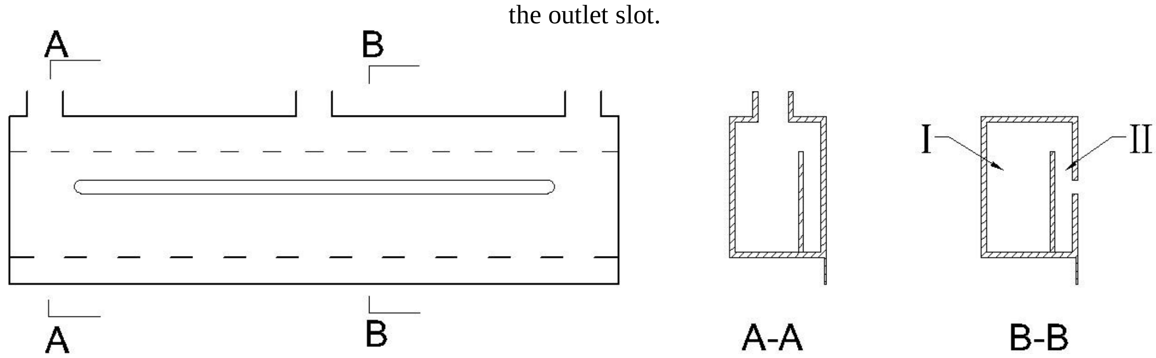

Fig.3 Schematic of the solution distributor

In the experiment, the inlet parameters of process air, liquid desiccant solution and cooling water were controlled and adjusted. The air flow rate was controlled by the voltage regulator of the fan. The air temperature was regulated by the air heater with PID controller and the air humidity by the electromagnetic humidifier which was controlled by adjusting the input voltage. In addition, the solution flow rate was regulated by the valve installed at the outlet of the pump and the temperature was controlled by the heat exchanger fixed inside the solution tank.

The inlet and outlet parameters of process air, liquid desiccant solution and cooling water were measured for each test. The temperature was measured by platinum resistance temperature detectors (Pt RTDs). The air flow rate was measured by air velocity sensors with the accuracy of 0.3%. The desiccant solution and cooling water flow rates were measured by turbine flow rate sensors. The density of the desiccant aqueous solution was measured by a specific gravity hydrometer. Each test lasted for more than ten minutes under steady condition and the data was acquired by a data logger. The specifications of the measuring devices are listed in Table 1.

Table 1 Specifications of different measuring devices

Parameter	Device	Accuracy	Operational range
Air dry-/wet-bulb temperature	Pt RTD	0.1 K	223-573 K

Air flow rate	Air velocity sensor (ASF-100)	0.3%	9-10000 Pa
Solution temperature	Pt RTD	0.1 K	223-573 K
Solution flow rate	Turbine flow rate sensor	3%	0.5-7.5 L/min
Solution density	Specific gravity hydrometer (DH-300X)	1 kg/m^3	1-99, 999 kg/m^3
Cooling water temperature	Pt RTD	0.1 K	223-573 K
Cooling water flow rate	Turbine flow rate sensor	3%	0.5-7.5 L/min

The nanoscale TiO_2 superhydrophilic coating was applied in the experiment to improve the surface wettability of the substrate plate. The primary size of the TiO_2 superhydrophilic particles was ac.5 nm and the particle was dispersed by 1 mm ZrO_2 beads through the ball mill process by adding the suitable dispersant and stable agent. The solvent of the TiO_2 superhydrophilic coating solution was ethanol and the concentration was 1%. The stainless steel plate was prewashed with ethanol before the coating process. Then the nanoscale TiO_2 superhydrophilic coating solution was evenly sprayed on the plate surface. Lastly, the coated plate was activated by ultraviolet light for 2 hours before test.

3. Performance indices, uncertainty analysis and results validation

In the experiment, the extra moisture was removed from the process air to the liquid desiccant due to the surficial vapor pressure difference. To evaluate the dehumidification performance of the plate dehumidifiers, three performance indices, the moisture removal rate m_{ω}, the dehumidification efficiency η_{ω} and the mass transfer coefficient h_{D} were introduced in this paper. In addition, the performance enhancing ratio ε was proposed to compare the dehumidification performance of the coated and uncoated plate dehumidifiers.

The moisture removal rate m_{ω} represents the moisture handling capacity of the plate dehumidifier and is defined as follows.

$$m_{\omega} = m_{\mathrm{a}}(\omega_{\mathrm{a,in}} - \omega_{\mathrm{a,out}}) \quad (1)$$

Where m_{a} is the mass flow rate of air, kg/s. $\omega_{\mathrm{a,in}}$ and $\omega_{\mathrm{a,out}}$ represent the inlet and outlet air humidity, g/kg dry air, respectively.

The dehumidification efficiency η_{ω} is defined as the ratio of the actual moisture change between process air and liquid desiccant to the maximum possible change. η_{ω} can be calculated as follows.

$$\eta_{\omega} = \frac{\omega_{\mathrm{a,in}} - \omega_{\mathrm{a,out}}}{\omega_{\mathrm{a,in}} - \omega_{\mathrm{equ,in}}} \quad (2)$$

Where $\omega_{\mathrm{equ,in}}$ represents the air absolute humidity in equilibrium with the inlet solution at its temperature and concentration, g/kg dry air.

The mass transfer coefficient h_D represents the mass transfer rate between process air and liquid desiccant solution, $g/(m^2 \cdot s)$.

$$h_D = \frac{m_a(\omega_{a,in} - \omega_{a,out})}{A\Delta\omega} \quad (3)$$

Where A is the wetting area of the falling film, m^2, and $\Delta\omega$ is the mean humidity difference between process air and desiccant solution, g/kg dry air.

The performance enhancing ratio is defined as the ratio of the dehumidification performance, including moisture removal rate and dehumidification efficiency, of the coated plate dehumidifier to that of the uncoated one.

$$\varepsilon_\omega = \frac{m_{\omega,\ coated}}{m_{\omega,\ uncoated}} \quad (4)$$

$$\varepsilon_\eta = \frac{\eta_{\omega,\ coated}}{\eta_{\omega,\ uncoated}} \quad (5)$$

Where ε_ω and ε_η represent the enhancing ratios of moisture removal rate and dehumidification efficiency.

As the measuring errors exists in the experimental setup, the uncertainty analysis of the experimental results is necessary. The uncertainty analysis was conducted by using the uncertainty propagation method [27], as shown in Equation (6).

$$\delta U = \sqrt{(\frac{\partial U}{\partial x_1}\delta x_1)^2 + (\frac{\partial U}{\partial x_2}\delta x_2)^2 + (\frac{\partial U}{\partial x_3}\delta x_3)^2 + \cdots + (\frac{\partial U}{\partial x_n}\delta x_n)^2} \quad (6)$$

Where δU is the uncertainty of the calculated parameter U. δx_1, δx_2 and δx_3 represent the absolute uncertainty of the measured values, x_1, x_2, x_3. According to Equation (6) and Table 1, the uncertainty of the moisture removal rate, dehumidification efficiency and mass transfer coefficient are 3.2%, 3.4% and 5.4%, respectively.

Before the experimental results analysis, the energy conservation analysis should be conducted to verify the reliability of the experimental results. Due to the temperature difference between liquid desiccant and process air as well as the phase change during the dehumidification process, heat transfer occurred between process air, liquid desiccant and cooling water. Therefore, the energy conservation equation are defined as follows.

$$m_a(h_{a,in} - h_{a,out}) = (m_{s,out}h_{s,out} - m_{s,in}h_{s,in}) + m_f C_{p,f}(T_{f,out} - T_{f,in}) \quad (7)$$

Fig. 3 shows the energy conservation conditions of the plate dehumidifier. It can be observed that most of the results evenly fell within ±30% error band, validating the accuracy of the experimental results. In addition, the heat released by the process air is a little higher than that absorbed by the liquid desiccant and the cooling water from Fig. 3. It could be explained that part of the heat was released to the surroundings despite the thermal insulation of the system.

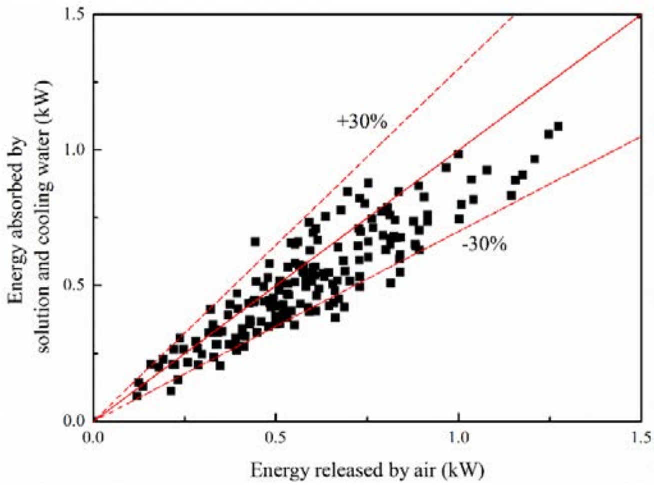

Fig. 3. Energy conservation of the experimental results

4. Results and discussion

4.1 Characterization of the TiO_2 superhydrophilic coating

As discussed above, the TiO_2 superhydrophilic coating was used in the experiment to improve the surface wettability. To characterize the superhydrophilic coating, Scanning Electron Microscope (SEM) test was conducted. Fig. 4 shows the SEM image of the nanoscale TiO_2 particles. In addition, to prevent the corrosion of the substrate plate caused by the LiCl aqueous solution, a double-layer structure of the coating with an inorganic compact protective layer beneath the TiO_2 coating was developed. The SEM images of the double-layer structure is shown in Fig. 5. Part Ⅰ, Ⅱ and Ⅲ represent the substrate plate, the inorganic compact protective layer and the TiO_2 superhydrophilic layer, respectively. As the TiO_2 superhydrophilic layer and the protective layer were much thinner than the stainless steel plate, the thermal conductivity of the coating was ignored.

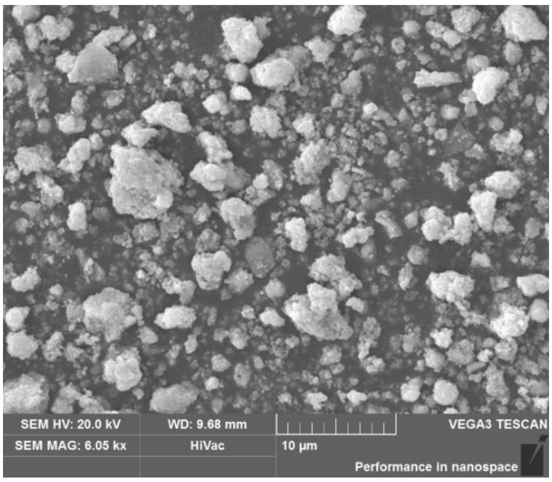

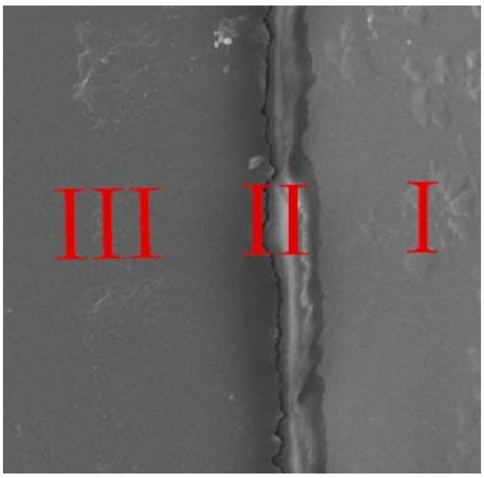

Fig. 4. SEM image of the nanoscale TiO_2 particles **Fig. 5.** SEM image of the double-layer structure

The wettability of the solid surface can be characterized by the contact angle. Contact angle measurement was performed by a contact angle goniometer and the standard sessile drop method was adopted in the test. Fig. 6 shows the contact angles of the desiccant aqueous solution on the coated and uncoated surface. It can be clearly observed that the contact angles of the liquid desiccant drops significantly from 84.6° on the uncoated plate to 8.8° on the coated one. The test resutls indicated that the wettability of the solid surface could be effectively improved with the TiO_2 superhydrophilic coating.

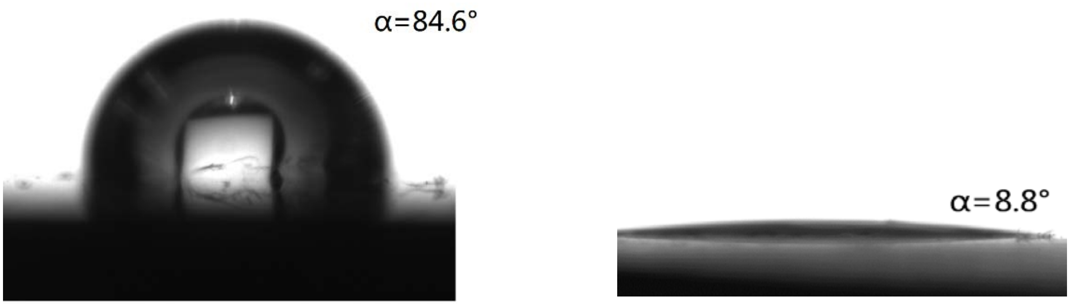

(a) Uncoated plate (b) Coated plate

Fig. 6. Contact angles of LiCl aqueous solution on the coated and uncoated plates

4.2 Dehumidification performance enhancement

In the experiment, more than 200 experimental conditions were selected based on Hong Kong climate to investigate the dehumidification performance enhancement with TiO_2 superhydrophilic coating. The detailed ranges of the experimental conditions are listed in Table 2 and part of the experimental conditions were listed in Table 3.

Table 2 Detailed ranges of the inlet experimental parameters

$T_{a,in}$ (℃)	$\omega_{a,in}$ (g/kg)	$m_{a,in}$ (kg/s)	$T_{s,in}$ (℃)	$m_{s,in}$ (kg/s)	$T_{f,in}$ (℃)	m_f (kg/s)
23.6-38.7	10.9-26.2	0.027-0.07	23.1-30.5	0.01-0.049	15.6-24.9	0.03-0.10

Table 3 Part of the experimental conditions for coated and uncoated plate dehumidifiers

No.	$T_{a,in}$ (℃)	$T_{a,out}$ (℃)	$\omega_{a,in}$ (g/kg)	$\omega_{a,out}$ (g/kg)	$T_{s,in}$ (℃)	$T_{s,out}$ (℃)	$T_{f,in}$ (℃)	$T_{f,out}$ (℃)	m_a (kg/s)	m_s (kg/s)
1	26.5	26.8	19.4	14.7	26.4	28	16.5	17.2	0.062	0.044
2	29.0	28.0	19.4	15.0	26.3	27.9	16.4	17.3	0.062	0.045
3	30.1	28.9	23.6	17.5	25.8	28.1	15.7	17.0	0.061	0.044
4	33.8	30.4	23.8	18.3	25.9	28.3	16.0	17.3	0.061	0.044
5	29.7	28.0	13.5	11.0	23.9	27.3	15.8	16.5	0.063	0.015
6	29.6	28.2	13.6	11.8	23.8	29.4	16.1	16.6	0.063	0.010
7	29.5	29.0	17.6	14.5	27.0	30.5	16.8	17.5	0.063	0.016
8	29.5	29.0	17.7	15.6	27.4	32.6	15.9	17.0	0.063	0.010
9	30.1	28.9	22.6	17.3	26.3	28.9	16.8	18.3	0.057	0.047

10	30.3	28.6	22.7	17.5	26.7	28.2	16.1	17.2	0.049	0.045
11	29.7	26.3	20.2	15.5	25.2	27.2	20.2	20.8	0.061	0.043
12	30.1	26.2	19.9	16.0	25.8	27.2	23.0	23.3	0.061	0.048

Fig. 7 presents the probability density of the performance enhancing ratios of the coated dehumidifier. The dehumidification performance was significantly enhanced by the TiO_2 superhydrophilic coating. Both enhancing ratios increased from 1.0 to 2.4 with the mean values of 1.60 and 1.63 for ε_ω and ε_η, respectively. To further analyse the data, Gauss curves were fitted in the figure. The results demonstrated that the highest probability for the enhancing ratios lied in 1.5. The performance enhancement of the coated plate dehumidifier can be attributed to the increase of the wetting area and the decrease of the falling film thickness caused by the TiO_2 superhydrophilic coating. As discussed above, the contact angle of the liquid desiccant on the working plates was significantly reduced by the coating, which could effectively prevent the shrinkage of the falling film and therefore increase the wetting area. In addition, the falling film thickness on the coated plate also decreased with the increase of the surface wettability. The decrease of the falling film thickness could benefit the dehumidification performance by reducing the heat transfer resistance between the falling film and the cooling water. Besides, the mass transfer resistance inside the falling film could also be reduced by accelerating the replenishment of the surficial liquid desiccant.

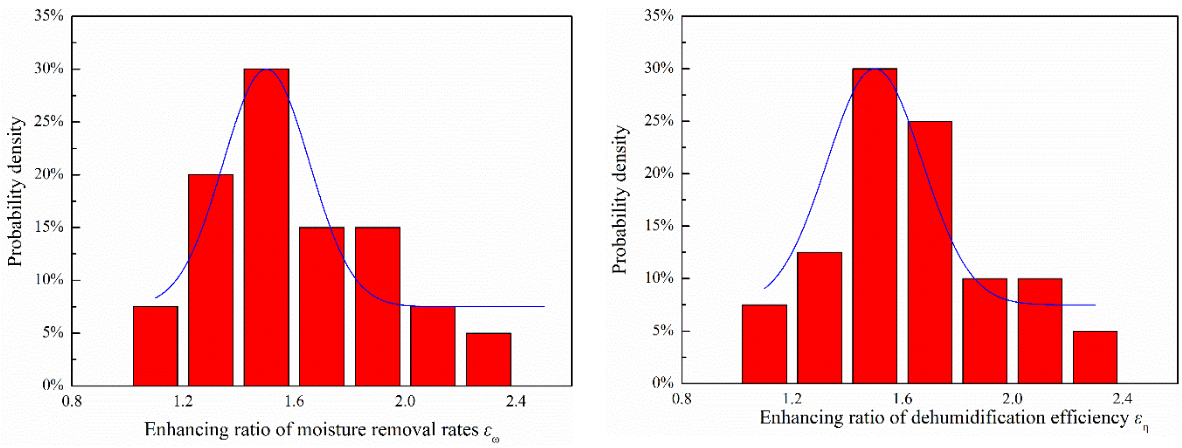

(a) Enhancing ratio of moisture removal rate ε_ω (b) Enhancing ratio of dehumidification efficiency ε_η

Fig. 7. Probability density of the performance enhancing ratio for the coated plate dehumidifier.

4.3 Influencing factors analysis of the dehumidification performance

The influence of the inlet parameters (including air temperature, air humidity and air flow rate, desiccant flow rate and cooling water temperature) on the dehumidification performance for the coated and uncoated plate dehumidifiers was investigated comprehensively in this section.

4.3.1 Effect of air temperature

Fig. 8 shows the variation of dehumidification performance with air temperature at different inlet air humidity for the coated and uncoated plate dehumidifiers. It can be clearly observed that dehumidification performance of the coated plate dehumidifier was much better than that of the uncoated plate dehumidifier. Both the moisture removal rate and the dehumidification efficiency decreased with the increase of air temperature. As air temperature increased, more heat was exchanged from the air to the liquid desiccant. The temperature increase of the liquid desiccant could reduce the driving force of the dehumidification process and therefore deteriorate the dehumidification performance. Another interesting finding from Fig. 8 is that the dehumidification performance of the uncoated plate dehumidifier dropped more rapidly than that of the coated one. It was found that the temperature increase of the liquid desiccant at the surface was much bigger with higher air temperature in uncoated plate dehumidifier, which hindered the absorption process. However, in coated plate dehumidifier, the heat absorbed by the surficial liquid desiccant could be quickly passed to the liquid desiccant inside and then to the cooling water due to thinner falling film thickness.

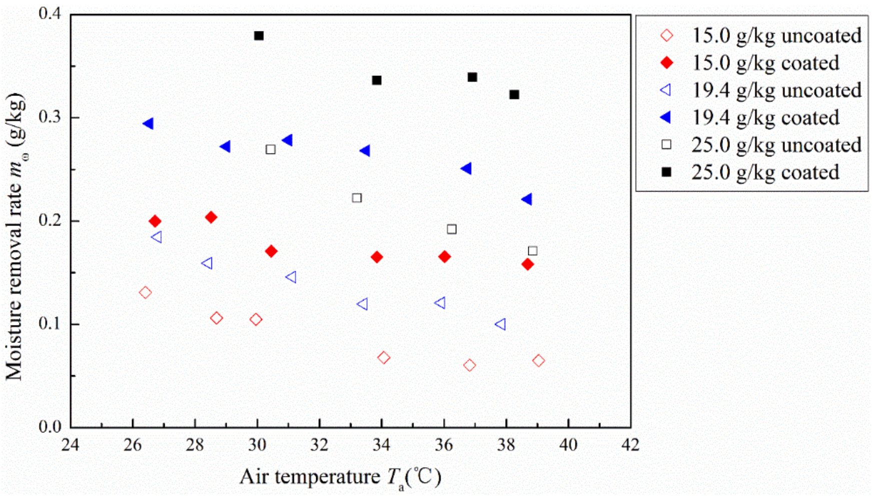

(a) Moisture removal rate m_ω

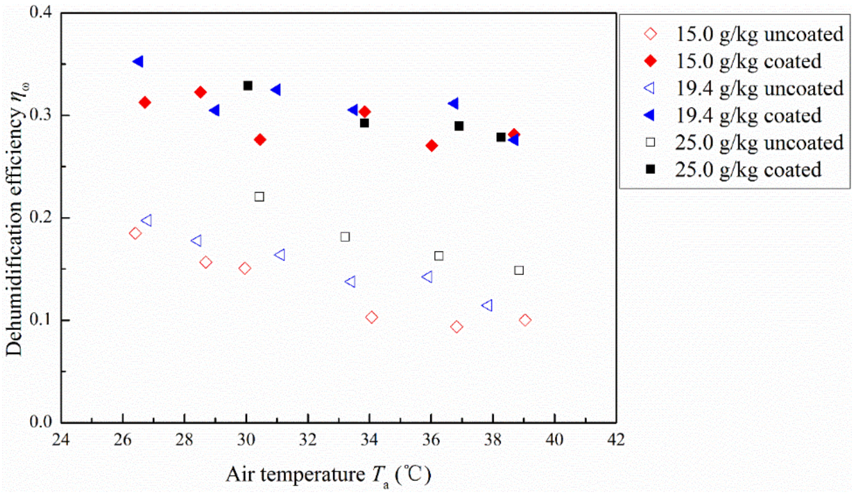

(b) Dehumidification efficiency η_ω

$T_{a,in}$ (℃)	$\omega_{a,in}$ (g/kg)	$m_{a,in}$ (kg/s)	$T_{s,in}$ (℃)	$m_{s,in}$ (kg/s)	$T_{f,in}$ (℃)	m_f (kg/s)
26.4-38.7	15.0, 19.4, 25.0	0.06	26.4	0.043	20.0	0.050

Fig. 8. Effect of air temperature on dehumidification performance of coated and uncoated plate dehumidifiers.

4.3.2 Effect of air humidity

Fig. 9 demonstrates the effect of air humidity on dehumidification performance. As the air humidity varies a lot during the whole year, it is necessary to investigate the effect of air humidity on dehumidification performance. As shown in Fig. 9(a), the moisture removal rate increased rapidly with the air humidity. The driving force of the vapor absorption increased significantly with the air humidity, which led to obvious increase of the moisture removal rate. However, as shown in Fig. 9(b), the dehumidification efficiency just increased slightly with air humidity. As air humidity increased, both the actual moisture absorption rate and the maximum possible one increased accordingly. The compromising results led to a slight increase of the dehumidification efficiency.

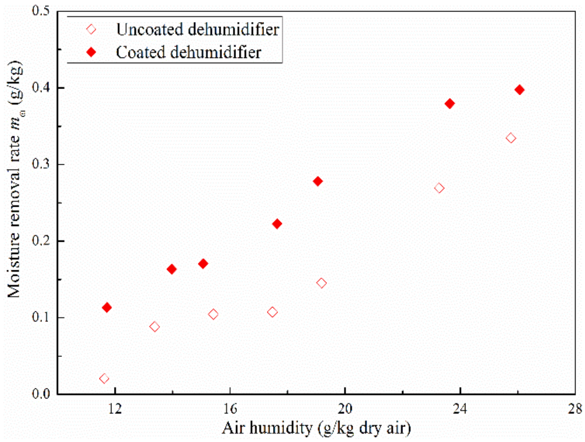

(a) Moisture removal rate m_ω

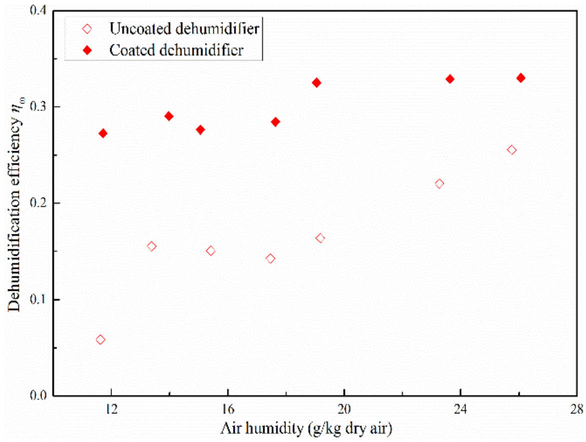

(b) Dehumidification efficiency η_ω

$T_{a,in}$ (℃)	$\omega_{a,in}$ (g/kg)	$m_{a,in}$ (kg/s)	$T_{s,in}$ (℃)	$m_{s,in}$ (kg/s)	$T_{f,in}$ (℃)	m_f (kg/s)
30.5	11.7-26.2	0.06	26.1	0.043	20.0	0.050

Fig. 9. Effect of air humidity on dehumidification performance of coated and uncoated plate dehumidifiers.

4.3.3 Effect of air flow rate

The influence of air flow rate on dehumidification performance for the coated and uncoated plate dehumidifier is shown in Fig. 10. The moisture removal rate increased monotonously while the dehumidification efficiency decreased slightly with air flow rate. As the length of the plate dehumidifier is limited, the increase of air flow rate might lead to insufficient contact time for the air and liquid desiccant. Therefore, the dehumidification efficiency dropped with air flow rates.

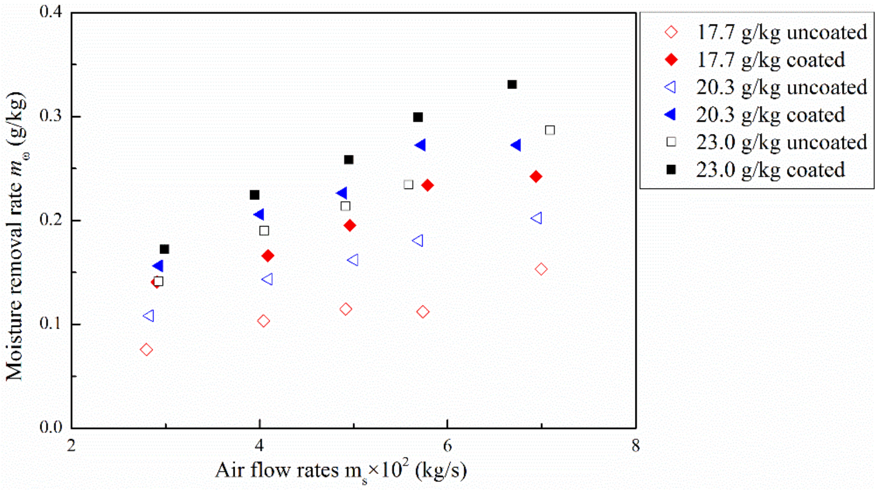

(a) Moisture removal rate m_ω

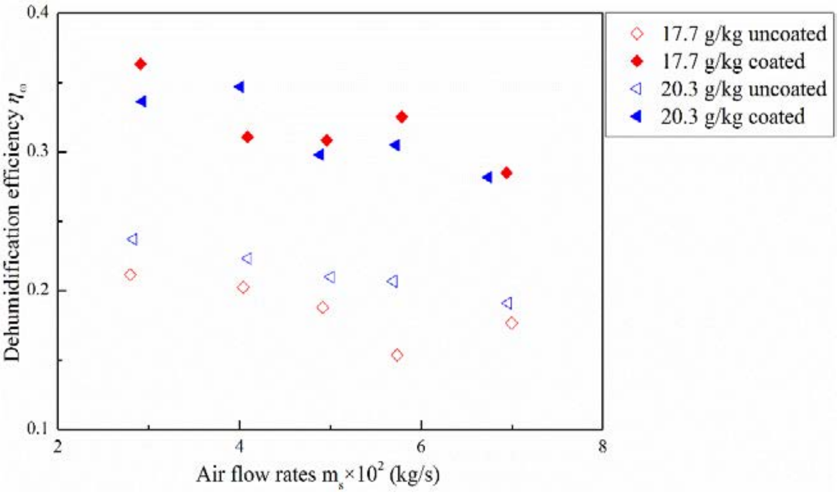

(b) Dehumidification efficiency η_ω

$T_{a,in}$ (℃)	$\omega_{a,in}$ (g/kg)	$m_{a,in}$ (kg/s)	$T_{s,in}$ (℃)	$m_{s,in}$ (kg/s)	$T_{f,in}$ (℃)	m_f (kg/s)
30.5	17.7, 20.3, 23	0.029-0.069	26.0	0.043	20.0	0.050

Fig. 10. Effect of air flow rate on dehumidification performance of coated and uncoated plate dehumidifiers.

4.3.4 Effect of desiccant solution flow rate

Fig. 12 presents the variation of the wetting ratios with the desiccant flow rates for the coated and uncoated plate dehumidifiers. The wetting ratio represents the ratio of the actual wetting area to the maximum possible one. It was clearly observed that the wetting ratio on the coated plate was much higher than that on the uncoated one. Due to the shrinkage of the falling film, the maximum wetting ratio on the uncoated plate was below 75%. However, the coated plate was easy to be completely or almost completely wetted by the desiccant solution. That was because the TiO_2 superhydrophilic coating on coated plate could significantly increase surface wettability and reduce the shrinkage of the falling film. In addition, both the wetting ratios on the coated and uncoated plate firstly increased rapidly and then slightly with the solution flow rates. Falling film breakdown occurred at low solution flow rates and increasing the flow rates could effectively reduce the breakdown and therefore significantly increase the wetting ratios. One interesting finding was that the minimum wetting flow rate on the coated plate was 0.015 kg/s which was lower than that on the uncoated plate with the value of 0.020 kg/s. The minimum wetting flow rate represents the minimum required solution flow rate to avoid the falling film breakdown. The difference was attributed to the higher surface wettability on the coated plate.

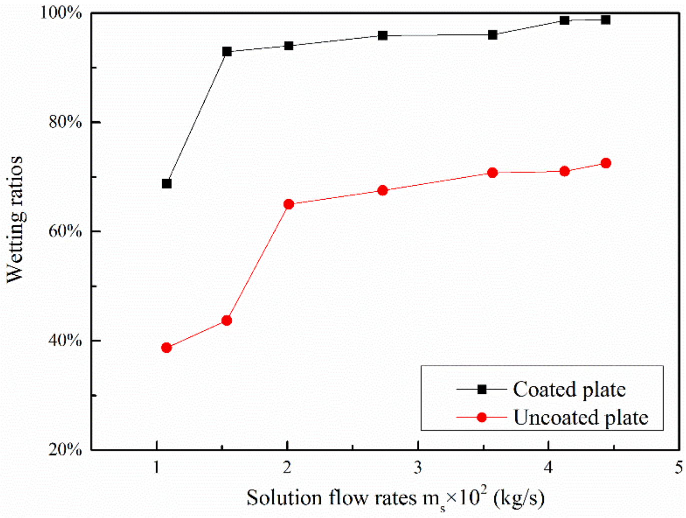

Fig. 12 Effect of solution flow rates on wetting ratios on coated and uncoated plates

As shown in Fig. 11, both the moisture removal rate and the dehumidification efficiency increased with desiccant flow rates. Firstly, the wetting area of the liquid desiccant increased with desiccant flow rates, which could directly improve the dehumidification performance. Secondly, the fluctuation of the liquid desiccant falling film was also enhanced with higher desiccant flow rates. The higher fluctuation could accelerate the replenishment of the surficial liquid desiccant and reduce the mass transfer resistance inside the falling film. Lastly, the temperature increase of the liquid desiccant was reduced with higher desiccant flow rates. The experimental results indicated that the temperature increase of the liquid desiccant was reduced from 3.6℃ to 1.7℃ as the desiccant flow rate increased from 0.16 g/kg to 0.045 g/kg. One interesting finding from Fig. 11(a) is that the moisture removal rate firstly increased rapidly then slightly with desiccant flow rates, which can be explained by the variation of the wetting area with the solution flow rates, as shown in Fig. 12. The increase of desiccant flow rate could significantly increase the wetting area and therefore significantly increase the dehumidification performance with lower desiccant flow rates. As desiccant flow rate increased above the minimum wetting flow rate, the wetting area just increased slightly, leading to a slight increase of the dehumidification performance.

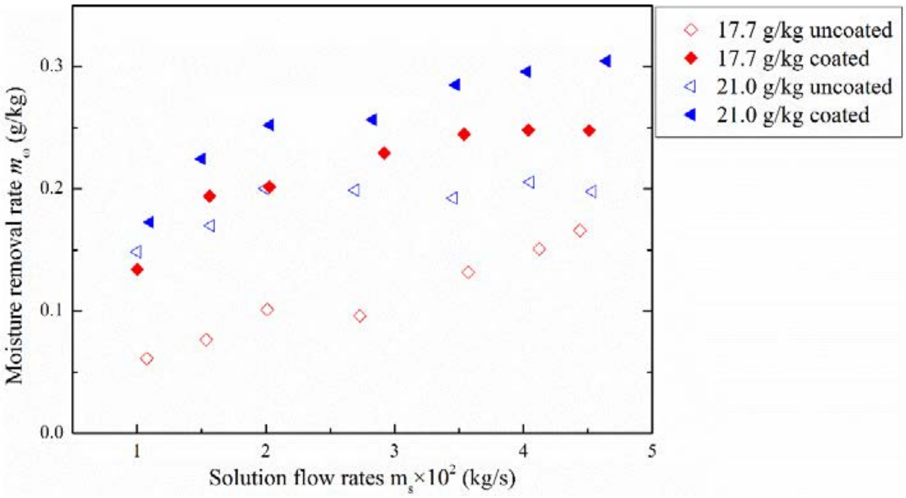

(a) Moisture removal rate m_ω

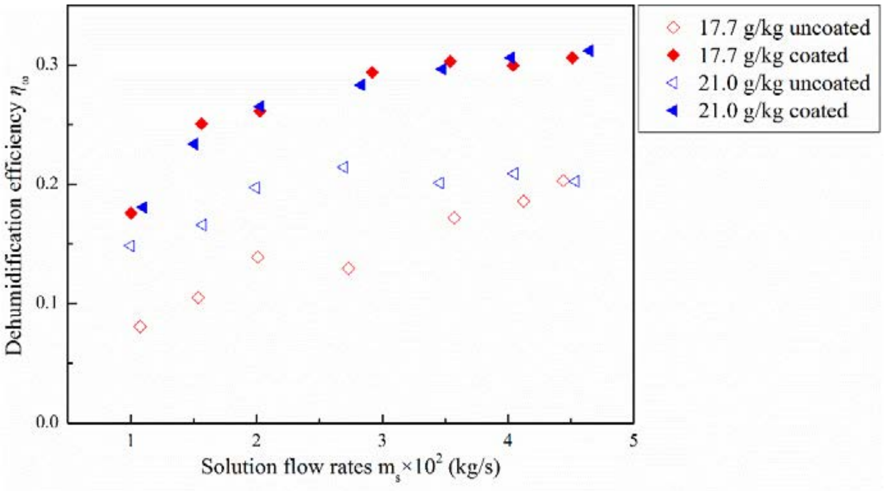

(b) Dehumidification efficiency η_ω

$T_{a,in}$ (℃)	$\omega_{a,in}$ (g/kg)	$m_{a,in}$ (kg/s)	$T_{s,in}$ (℃)	$m_{s,in}$ (kg/s)	$T_{f,in}$ (℃)	m_f (kg/s)
30.3	17.7, 21.0	0.06	25.9	0.01-0.049	20.1	0.050

Fig. 11. Effect of desiccant flow rate on dehumidification performance of coated and uncoated plate dehumidifiers.

4.3.5 Effect of cooling water temperature

In internally-cooled liquid desiccant dehumidifier, the cooling water is used to remove the latent heat released during the absorption process and to prevent the temperature increase of the liquid desiccant. Therefore, the cooling water temperature is very important to dehumidification performance. Fig. 12 illustrates the effect of cooling water temperature on dehumidification performance of coated and uncoated plate dehumidifiers. Both the moisture removal rate and the dehumidification efficiency decreased with increase of the cooling water temperature. The temperature increase deteriorated the heat transfer between the cooling water and the desiccant solution and therefore affected the dehumidification performance. In addition, vapor condensation might occur on the exposed surface in some experimental conditions with high humidity and low cooling water temperature, which could also enlarge the dehumidification rate.

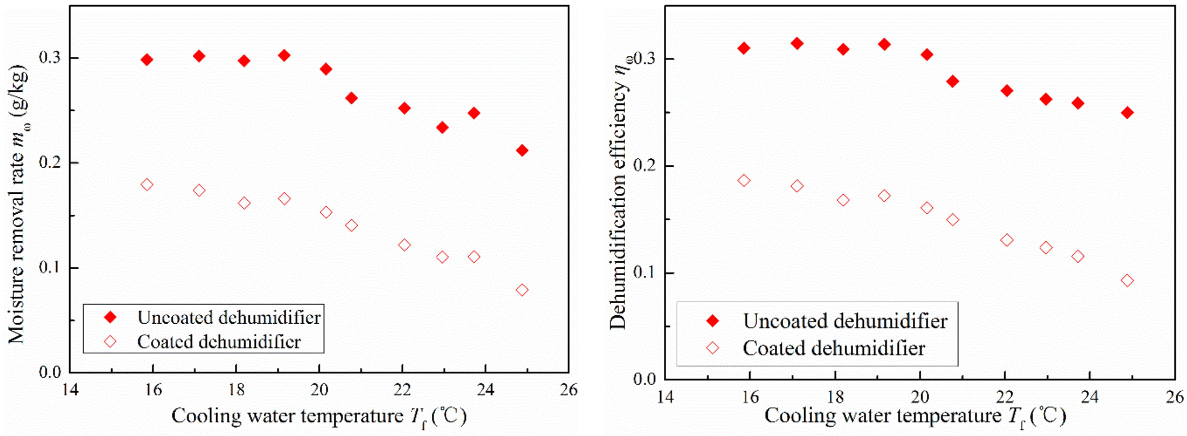

(a) Moisture removal rate m_ω (b) Dehumidification efficiency η_ω

$T_{a,in}$ (℃)	$\omega_{a,in}$ (g/kg)	$m_{a,in}$ (kg/s)	$T_{s,in}$ (℃)	$m_{s,in}$ (kg/s)	$T_{f,in}$ (℃)	m_f (kg/s)
30.1	20.2	0.06	26	0.043	15.8-24.9	0.050

Fig. 12. Effect of cooling water temperature on dehumidification performance of coated and uncoated plate dehumidifiers.

4.4 Fitting formula of mass transfer coefficient

Based on the experimental results above, the empirical correlations of mass transfer coefficient for the coated and uncoated plate dehumidifiers were developed using nonlinear regression. The mass transfer coefficient was calculated by Equation (3). Thus, the empirical correlations for the coated and uncoated plate dehumidifiers were presented as below.

For uncoated plate dehumidifier

$$h_D = 7.98 \times 10^4 \times m_a^{0.686} \times m_s^{0.250} \times T_a^{-1.78} \times T_f^{-0.527} \times \omega_a^{0.996} \quad (8)$$

For coated plate dehumidifier

$$h_D = 3.15 \times 10^4 \times m_a^{0.972} \times m_s^{0.229} \times T_a^{-0.379} \times T_f^{-0.375} \times \omega_a^{0.012} \quad (9)$$

. Fig. 13 presents the comparisons between the predicted mass transfer coefficients using the new correlations and the experimental results for the coated and uncoated plate dehumidifiers. Most of the predicted results fell within ±25% error band of the experimental results and the average relative derivation error was -0.9% and -1.09% for the coated and uncoated plate dehumidifiers respectively, thereby validating the new correlations.

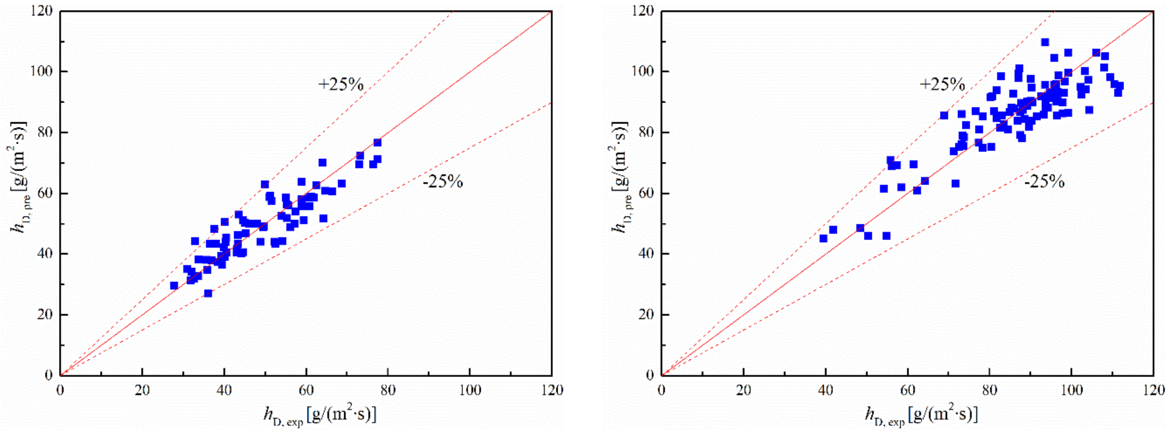

(a) Uncoated plate dehumidifier (b) Coated plate dehumidifier

Fig. 13. Comparisons between the predicted mass transfer coefficients and the experimental results.

5 Energy consumption analysis of LDAC system with coated plate dehumidifiers

To further estimate the performance of the coated plate dehumidifier with TiO_2 superhydrophilic coating, the energy consumption of the LDAC system with coated and uncoated plate dehumidifiers for a typical commercial building in Hong Kong was simulated and analysed. The detail of the building can be referenced in Qi et al. [28]. Fig. 14 shows the annual electricity consumption of the LDAC system with coated and uncoated plate dehumidifiers, respectively. Four main parts are considered in LDAC system, including the regenerator, the chiller, the pump and the fan. The simulation results indicated that nearly 80 MW·h of the electricity consumption can be saved with the coated plate dehumidifier compared with that with the uncoated one. In addition, the main energy saving lay in the chillers. The reason was that the dehumidification performance was significantly improved with the TiO_2 superhydrophilic coating, which reduced the latent load of the system.

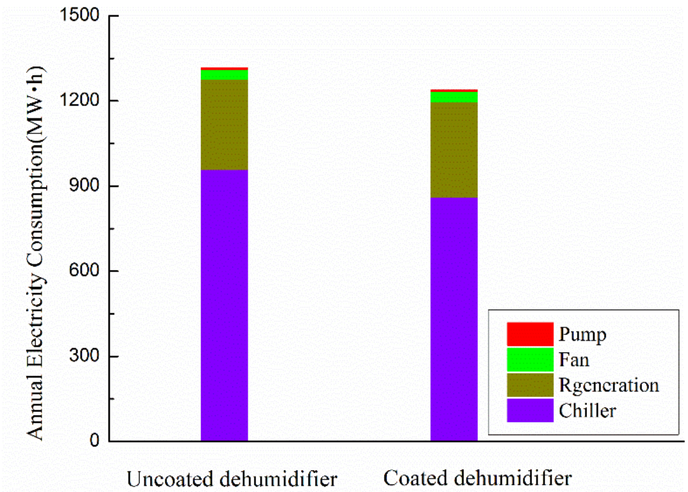

Fig. 14. Annual electricity consumption of plate LDAC system with coated and uncoated dehumidifiers

6. Conclusions

In this paper, a novel TiO_2 superhydrophilic coating was applied in liquid desiccant plate dehumidifiers to enhance the dehumidification performance. The experimental analysis indicated that the dehumidification performance could be effectively improved by the superhydrophilic coating. The main conclusions are drawn as follows.

(1) A double layer TiO_2 superhydrophilic coating was developed and the characterization of the coating was conducted. The test results showed that the contact angle of the liquid desiccant was significantly reduced from 84.6° to 8.8° and the surface wettability was effectively enhanced by the superhydrophilic coating.

(2) The dehumidification performance, including moisture removal rate ε_ω and dehumidification efficiency ε_η, was significantly improved with the TiO_2 superhydrophilic coating. The average enhancing ratios for ε_ω and ε_η were 1.60 and 1.63, respectively. The performance enhancement was mainly attributed to the increase of wetting area and the decrease of falling film thickness.

(3) The influencing factors of the dehumidification performance were analysed experimentally. A new empirical correlation of mass transfer coefficient was developed based on the experimental results using nonlinear regression method. The effect of surface wettability was considered by adding the contact angles in the new correlation.

(4) The energy consumption of the LDAC systems with coated and uncoated plate dehumidifiers for a commercial building in Hong Kong was simulated and analysed. The simulation results indicated that around 80 $MW\cdot h$ of the electricity consumption could be saved with the TiO_2 superhydrophilic coating.

Acknowledgements

This work was supported by the RGC General Research Fund (PolyU 152010/15E) and The Hong Kong Polytechnic University through Central Research Grant (PolyU 152110/14E).

References

[1] P. Tuominen, R. Holopainen, L. Eskola, J. Jokisalo, M. Airaksinen, Calculation method and tool for assessing energy consumption in the building stock, Building and Environment. 75 (2014) 153-160.

[2] L. Pérez-Lombard, J. Ortiz, J.F. Coronel, I.R. Maestre, A review of HVAC systems requirements in building energy regulations, Energy and Buildings. 43 (2-3) (2011) 255-268.

[3] Hong Kong Energy End-Use Data, Electrical and Mechanical Services Department of Hong Kong Special Administrative Region, 2013. http://www.emsd.gov.hk/emsd/e_download/pee/HKEEUD2013.pdf.

[4] T. Zhang, X.H. Liu, J.J. Jiang, X. Chang, Y. Jiang, Experimental analysis of an internally-cooled liquid desiccant dehumidifier, Building and Environment. 63 (2013) 1-10.

[5] M. Tu, C.Q. Ren, G.F. Tang, Z.S. Zhao, Performance Comparison between two novel configurations of liquid desiccant air-conditioning system, Building and Environment. 45 (12) (2010) 2808-2816.

[6] J.P. Pohl, H.M. Hellman, G. Grossman, Investigation and comparison of two configurations of a novel open-cycle absorption chiller, International Journal of Refrigeration. 21 (2) (1998) 142-149.

[7] X.H. Liu, X.M. Chang, J.J. Xia, Y. Jiang, Performance analysis on the internally cooled dehumidifier using liquid desiccant, Building and Environment. 44 (2) (2009) 299-308.

[8] Y.G. Yin, X.S. Zhang, Z. Chen, Experimental study on dehumidifier and regenerator of liquid desiccant cooling air conditioning system, Building and Environment. 42 (2007) 2505-2511.

[9] J. Liu, T. Zhang, X.H. Liu, J.J. Jiang, Experimental analysis of an internally-cooled/heated liquid desiccant dehumidifier/regenerator made of thermally conductive plastic, Energy and Buildings. 99 (2015) 75-86.

[10] Y.M. Luo, S.Q. Shao, H.B. Xu, C.Q. Tian, H.X. Yang, Experimental and theoretical research of a fin-tube type internally-cooled liquid desiccant dehumidifier, Applied Energy. 133 (2014) 127-134.

[11] X.H. Liu, Z. Li, Y. Jiang, Similarity of coupled heat and mass transfer between air-water and air-liquid desiccant direct-contact systems, Building and Environment. 44 (12) (2009) 2501-2509.

[12] Y.G. Yin, X.S. Zhang, Comparative study on internally heated and adiabatic regenerators in liquid desiccant air conditioning system, Building and Environment. 45 (2010) 1799-1807.

[13] R. Yang, D. Jou. Heat and mass transfer of absorption process for the falling film flow inside a porous medium, International Journal of Heat and Mass Transfer. 38 (6) (1995) 1121-1126.

[14] J.K. Kim, C.W. Park, Y.T. Kang, The effect of micro-scale surface treatment on heat and mass transfer performance for a falling film H_2O/LiBr absorber, International Journal of Refrigeration. 26 (5) (2003) 575-585.

[15] M. Yin, J.B. Chen, P. Chen, X.H. Ma, S.P. Li, Study on the heat-mass transfer in falling film outside the vertical tube for water vapor absorption into aqueous lithium bromide, Journal of Chemical Engineering of Chinese Universities. 16 (6) (2002) 604-608.

[16] Y. Zheng, X.H. Ma, Y. Li, R. Jiang, K. Wang, Z. Lan, Q.Q. Liang, Experimental study of falling film evaporation heat transfer on superhydrophilic horizontal-tubes at low spray density, Applied Thermal Engineering. 111 (2017) 1548-1556.

[17] C.S. Dong, L. Lu, R.H. Qi, Model development of heat/mass transfer for internally cooled dehumidifier concerning liquid film shrinkage shape and contact angles, Building and Environment, 114 (2017) 11-22.

[18] E. Hihara, T. Saito, Effect of surfactant on falling film absorption, International Journal of Refrigeration. 16 (5) (1993) 339-346.

[19] W.L. Cheng, K. Houda, Z.S. Chen, A. Akisawa, P. Hu, T. Kashiwagi, Heat transfer enhancement by additive in vertical falling film absorption of H_2O/LiBr, Applied Thermal Engineering. 24 (2-3) (2004) 281–298.

[20] B.H. Kang, K.H. Kim, D.Y. Lee, Fluid flow and heat transfer on a falling liquid film with surfactant from a heated vertical surface, Journal of Mechanical Science and Technology. 21 (2007) 1807–1812.

[21] L. Hoffmann, I. Greiter, A. Wanger, V. Weiss, G. Alefeld, Experimental investigation of heat transfer in a horizontal tube falling film absorber with aqueous solutions of LiBr with and without surfactants, International Journal of Refrigeration. 19 (5) (1996) 331–341.

[22] X.H. Ma, F.M. Su, J.B. Chen, Y. Zhang, Heat and mass transfer enhancement of the bubble absorption for a binary nanpfluid, Journal of Mechanical Science and Technology. 21 (2007) 1813-1818.

[23] D. Patil, R. Kumar, F. Xiao, Wetting enhancement of polypropylene plate for falling film tower application, Chemical Engineering and Processing: Process Intensification. 108 (2016) 1-9.

[24] B.P. Schwarzer, M.S. Rahbar, P. LeGoff, A spiral fin tube: a novel type of falling film heat and mass exchanger, International Absorption Heat Pump Conference, AES, 31 (1993) 179–183.

[25] M.R. Islam, N.E. Wijeysundera, J.C. Ho, Performance study of a falling-film absorber with a film-inverting configuration, International Journal of Refrigeration, 26 (8) (2003) 909-917.

[26] X.Y. Cui, J.Z. Shi, C. Tan, Investigation of plate falling film absorber with film-inverting configuration, Journal of Heat Transfer. 131 (7) (2009) 072001-1-9.

[27] H.W. Coleman, W.G. Steele, Experimentation, Validation and Uncertainty Analysis for Engineers, John Wiley & Sons, Inc., 2009.

[28] R.H. Qi, L. Lu, Energy consumption and optimization of internally cooled/heated liquid desiccant air-conditioning system: a case study in Hong Kong, Energy. 73 (2014) 801-808.